# Fixed-Frequency Beam Steering of Microstrip Leaky-Wave Antennas Using Binary Switches

Debabrata K. Karmokar, *Member, IEEE*, Karu P. Esselle, *Fellow, IEEE*, and Stuart G. Hay, *Senior Member, IEEE*

***Abstract*—This paper presents a novel, easy-to-fabricate and operate, single-layer leaky-wave antenna (LWA) that is capable of digitally steering its beam at fixed frequency using only two values of bias voltages, with very small gain variation and good impedance matching while scanning. Steering the beam of LWAs in steps at a fixed frequency, using binary switches, is investigated, and a new half-width microstrip LWA (HW-MLWA) is presented. The basic building block of the antenna is a reconfigurable unit cell, switchable between two states. A macrocell is created by combining several reconfigurable unit cells, and the periodic LWA is formed by cascading identical macrocells. A prototype HW-MLWA was designed, fabricated, and tested to validate the concept. To achieve fixed-frequency beam scanning, a gap capacitor in each unit cell is independently connected or disconnected using a binary switch. By changing the macrocell states, the reactance profile at the free edge of the microstrip and hence the main beam direction is changed. The prototyped antenna can scan the main beam between 31° and 60° at 6 GHz. The measured peak gain of the antenna is 12.9 dBi at 6 GHz and gain variation is only 1.2 dB.**

***Index Terms*—Binary switch, fixed-frequency beam steering, half-width (HW), leaky-wave antenna (LWA), macrocell, microstrip, reconfigurable.**

## I. Introduction

MICROSTRIP leaky-wave antennas (MLWAs) were originally demonstrated in the late 1970s [1] using the higher order mode of a microstrip line, with methods to excite that mode. The radiation properties of microstrip higher order modes gained rigorous research interest in the last decades [2], [3]. MLWAs are of particular practical interest because of their planar low-profile configuration, high gain, narrow beamwidth, large bandwidth, ease of fabrication, and beam-scanning capabilities [4]–[8]. These characteristics permit them to integrate easily with microwave and millimeter-wave circuits. The inherent beam-scanning capabilities of LWAs help to reduce the complexity of many systems that require beam-scanning facilities, such as automotive radar, multipoint communications, and surveillance [9].

Manuscript received May 21, 2015; revised February 16, 2016; accepted March 03, 2016. Date of publication March 25, 2016; date of current version May 30, 2016. This work was supported in part by the Australian Research Council (ARC) and in part by the International Postgraduate Research Scholarship (IPRS).

D. K. Karmokar and K. P. Esselle are with the Department of Engineering, Faculty of Science and Engineering, Macquarie University, Sydney, N.S.W. 2109, Australia (e-mail: dkkarmokar@ieee.org; karu@ieee.org).

S. G. Hay is with the CSIRO Digital Productivity Flagship, Marsfield, N.S.W. 2113, Australia (e-mail: Stuart.Hay@csiro.au).

Color versions of one or more of the figures in this paper are available online at http://ieeexplore.ieee.org.

Digital Object Identifier 10.1109/TAP.2016.2546949

The direction of the main beam of a LWA is given by [10]

$$\theta(f) = \sin^{-1}\left[\frac{\beta(f)}{k_0(f)}\right] \tag{1}$$

where $\beta$ is the phase constant, $k_0$ is the free-space wave number, and $\theta(f)$ is the angle from the boresight. In this case, the boresight is the direction perpendicular to the plane of the substrate. The value of $\beta/k_0$ changes with frequency, hence so does the beam direction. Different types of LWAs have been developed for beam scanning by changing the operating frequency [11]–[24]. In the fixed-frequency beam steering, $k_0$ is fixed, and hence, the effective $\beta$ should be changed by some other means without changing the frequency. For example, changing the reactance profile of a microstrip line changes the effective $\beta$ of the line and, hence, the beam direction [25].

Most communication systems operate in the predefined frequency bands. Often, these bands are relatively narrow, so scanning the beam at a fixed frequency is highly desirable [26], [27]. Several methods have been developed for beam scanning at a fixed frequency. One method is loading the leaky slots of a log-periodic LWA with lumped capacitors and changing their values [28]. Another demonstrated method is changing feed positions along an edge of a full-width multiterminal MLWA [29]. Beam scanning at a fixed frequency was demonstrated in [25] by loading the free edge of a half-width (HW)-MLWA with lumped capacitors, where 20 capacitors have been used to prove the concept. Electronic beam scanning has been achieved at a fixed frequency in [30] by varying the bias voltage of varactors in a one-dimensional (1-D) Fabry–Perot LWA. Predicted radiation patterns for a pattern-reconfigurable HW-MLWA is given in [31]. It uses a total of 35 lumped capacitors connected to the free edge of the microstrip. By changing the bias voltage of a varactor-loaded composite right/left-handed (CRLH) MLWA, the main beam has been steered at a fixed frequency [32]. Another method is to load an MLWA with a number of stubs at both edges of the microstrip [27]. Open-circuited and short-circuited stubs have been considered. Beam scanning at a fixed frequency would be possible if the spacing between adjacent stubs could be varied in this antenna.

A HW-MLWA proposed in [12] uses a septum (conducting wall) along the center of the microstrip to create an electric field null along the center line. This suppresses the fundamental mode and excites the first higher order mode. Uniform HW-MLWAs offer beam scanning by sweeping the operating frequency. Almost all the researches on HW-MLWAs are on frequency scanning; only limited research has been conducted to achieve beam steering at a fixed frequency from a HW-MLWA.

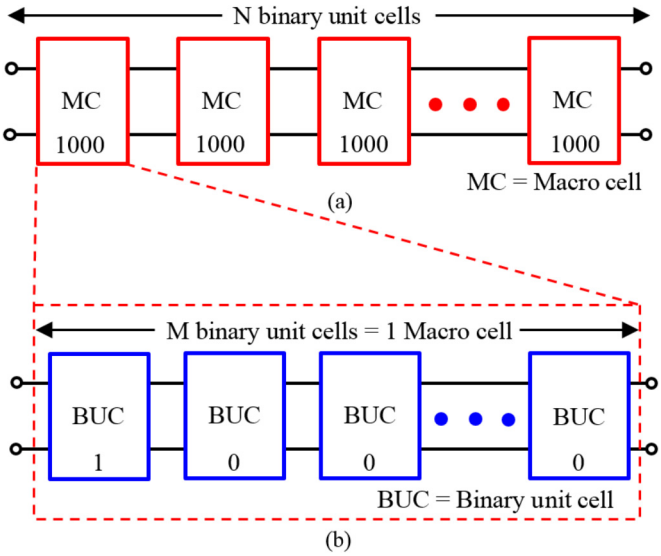


Fig. 1. Organization of cells in a 1-D reconfigurable periodic structure. (a) Macrocells into complete structure. (b) Unit cells into a macrocell.

In this paper, a technique to achieve fixed-frequency beam scanning from MLWAs is developed and a new HW-MLWA configuration, which does not require lumped capacitors, is proposed. Its novelty is two-fold: 1) in developing a systematic macrocell-based method to analyze and design digitally controlled reconfigurable electromagnetic devices including antennas, 2) in achieving high-quality impedance-matched beam scanning at a fixed frequency with very small gain variation, using only two values of bias voltages (required to turn the switches on and off) and a simple single-layer antenna that is easy to fabricate without lumped capacitors. The basic building block of the HW-MLWA is a binary reconfigurable unit cell, which is switchable between two states. For systematic analysis, several unit cells are combined to form a macrocell. The HW-MLWA is created by cascading several identical macrocells. The antenna beam is steered at a fixed frequency by changing the state of macrocells, as detailed in the next section. To validate the concept one antenna design has been prototyped and tested. A total of 24 unit cells are used in the prototype. A uniform frequency-scanning HW-MLWA is also investigated, for comparison with new antennas.

## II. Multistate Macrocells

The concept of creating a "larger cell" by cascading different types of unit cells has been studied previously for nonreconfigurable structures [15], [33]. Those large cells cannot be changed once the device is fabricated. Here, we present the concept of a bigger reconfigurable cell named "macrocell," which consists of reconfigurable unit cells, and the size and characteristics of the macrocell can be dynamically changed as detailed below.

Consider a 1-D periodic structure made out of reconfigurable binary unit cells. The state of each unit cell can be changed, independent of others, by a controlled binary switch in it. Each binary switch is in one out of two states, "ON" and "OFF," and these states are denoted hereafter as "1" and "0," respectively. Fig. 1 shows the generic configuration of a 1-D periodic structure, which consists of N such binary unit cells. Considering the periodicity of the complete binary pattern (CBP) across the structure, few unit cells are grouped into a "macrocell," and the whole structure is then represented as a cascade of identical macrocells as shown in Fig. 1(a). Each macrocell consists of M unit cells as shown in Fig. 1(b). In the periodic structure example shown in Fig. 1, the CBP is 100010001000. . ., which is obtained by repeating 1000. Hence, each macrocell is composed of four binary unit cells, which have the binary states of 1, 0, 0, and 0 in that order.

TABLE I
Binary Patterns of Macrocells and Corresponding CBPs of a 1-D Periodic Reconfigurable Structure (Every Other Macrocell is Highlighted)

| Macro-cell order | Macro-cell state | Macro-cell binary pattern | CBP along the sructure |
|---|---|---|---|
| M = 1 | M1(0) | 0 | 0000000000000.....0 |
| | M1(1) | 1 | 1111111111111.....1 |
| M = 2 | M2(0) | 00 | 0000000000000.....00 |
| | M2(1) | 01 | 0101010101010.....01 |
| | M2(2) | 10 | 1010101010101.....10 |
| | M2(3) | 11 | 1111111111111.....11 |
| M = 3 | M3(0) | 000 | 000000000000.....000 |
| | M3(1) | 001 | 001001001001.....001 |
| | M3(2) | 010 | 010010010010.....010 |
| | M3(3) | 011 | 011011011011.....011 |
| | M3(4) | 100 | 100100100100.....100 |
| | M3(5) | 101 | 101101101101.....101 |
| | M3(6) | 110 | 110110110110.....110 |
| | M3(7) | 111 | 111111111111.....111 |
| M = 4 | M4(0) | 0000 | 0000000000000.....0000 |
| | M4(1) | 0001 | 0001000100010.....0001 |
| | M4(2) | 0010 | 0010001000100.....0010 |
| | M4(3) | 0011 | 0011001100110.....0011 |
| | M4(4) | 0100 | 0100010001000.....0100 |
| | M4(5) | 0101 | 0101010101010.....0101 |
| | M4(6) | 0110 | 0110011001100.....0110 |
| | M4(7) | 0111 | 0111011101110.....0111 |
| | M4(8) | 1000 | 1000100010000.....1000 |
| | M4(9) | 1001 | 1001100110011.....1001 |
| | M4(10) | 1010 | 1010101010101.....1010 |
| | M4(11) | 1011 | 1011101110111.....1011 |
| | M4(12) | 1100 | 1100110011001.....1100 |
| | M4(13) | 1101 | 1101110111011.....1101 |
| | M4(14) | 1110 | 1110111011101.....1110 |
| | M4(15) | 1111 | 1111111111111.....1111 |

Let us define the order of a macrocell (M) as the number of unit cells in it. A macrocell can be considered as a multistate electromagnetic element with $2^M$ states. Binary patterns of four different orders of macrocells (M = 1, 2, 3, and 4) and corresponding CBPs for a periodic structure made out of 24 reconfigurable unit cells are listed in Table I. The jth state of the ith-order macrocell is denoted by Mi(j) as shown in the second column of Table I. The orders of macrocells (M) in Table I are chosen, such that all N cells in the structure can be represented by an integer number of macrocells, where M<<N, and $\frac{N}{M}$ is an integer. Although the CBP of N cells is periodic [e.g., 10001000. . .1000, as shown in Fig. 1(a)], the pattern within a macrocell [Fig. 1(b)] itself can be either periodic or aperiodic. For example, the binary pattern of the M4(4) macrocell state (in Table I) is 0100, which is not periodic. However, the pattern of the M4(5) macrocell state is 0101, which is periodic.

When this approach is applied for designing MLWAs and analyzing their radiation characteristics, the key factor is the complex propagation constant along the structure defined by $k = \beta - j\alpha$, where $\alpha$ is the attenuation constant. At a given frequency, each macrocell state has a corresponding average $\alpha$, average $\beta$, and, in the case of LWAs, a beam direction that is related to $\beta$ according to (1). Changing of macrocell states changes the average reactance profile along the microstrip line. It is well known that phase velocity and $\beta$ change with the reactance profile along the structure. At a fixed frequency, the two limits (upper and lower beam angle) of the beam scanning range are determined by the states of macrocells M1(0) and M1(1). Other beam directions within this range can be achieved, at the same frequency, by switching the LWA to other selected macrocell states.

For each periodic state of a higher order macrocell, it is possible to find one or more states of lower order macrocells with identical electromagnetic characteristics. For example, the EM properties of the M4(5) and M2(1) states are identical. In addition, shifting bits in a macrocell binary pattern does not change the EM characteristics significantly when N is sufficiently large. For example, M4(7), M4(11), M4(13), and M4(14) have practically the same EM characteristics. Therefore, M4(10), M4(5), M2(2), and M2(1) have nearly the same main beam direction at a fixed frequency. In other words, a lot of states are not unique and are practically redundant.

## III. Antenna Configurations

Fig. 2 shows the configuration of the proposed reconfigurable HW-MLWA consisting of binary switches. These antennas were designed and optimized using CST Microwave Studio. The length ($L$) and width ($W$) of the substrate are 266 mm ($5.32\lambda_0$) and 70 mm ($1.4\lambda_0$), respectively, where $\lambda_0$ is the free-space wavelength at 6 GHz. The length ($l$) and width ($w$) of the microstrip line are 240 mm ($4.8\lambda_0$) and 8 mm ($0.16\lambda_0$), respectively. The antenna prototype is printed on a Rogers RT5880 substrate with a thickness of 1.575 mm, dielectric constant of 2.2, and loss tangent of 0.0009. For comparison, the uniform HW-MLWA was modeled for the same substrate.

The antenna is made out of a HW microstrip line with one edge shorted to the ground plane by an array of vias. There are 24 unit cells in the reconfigurable antenna, each 10-mm long (i.e., $P$ = 10 mm). Each unit cell consists of a patch in the center of the cell, printed on the same surface as the microstrip. It is located very close to the free edge of the microstrip, leaving a narrow gap ($g$) of 0.1 mm between them [right inset of Fig. 2(a)], to form a gap capacitor. The dimensions of the patch are 3 mm × 4 mm ($w_p \times l_p$). The patch is connected to the ground plane by a via through a binary switch [Fig. 2(b)]. The outer diameter of the via ($d$) is 0.8 mm. The top edge of the via is connected to the patch, and the bottom edge is connected to a biasing pad printed on the same surface as the ground plane as shown in Fig. 2(b). The dimensions of the biasing pad are 3 mm × 3 mm. Two small pads, 1 mm × 1 mm each, called switch pads were designed to connect the switching-device pins [Fig. 2(b)]. One pad is connected to the biasing pad and the other is connected to the ground plane. There is

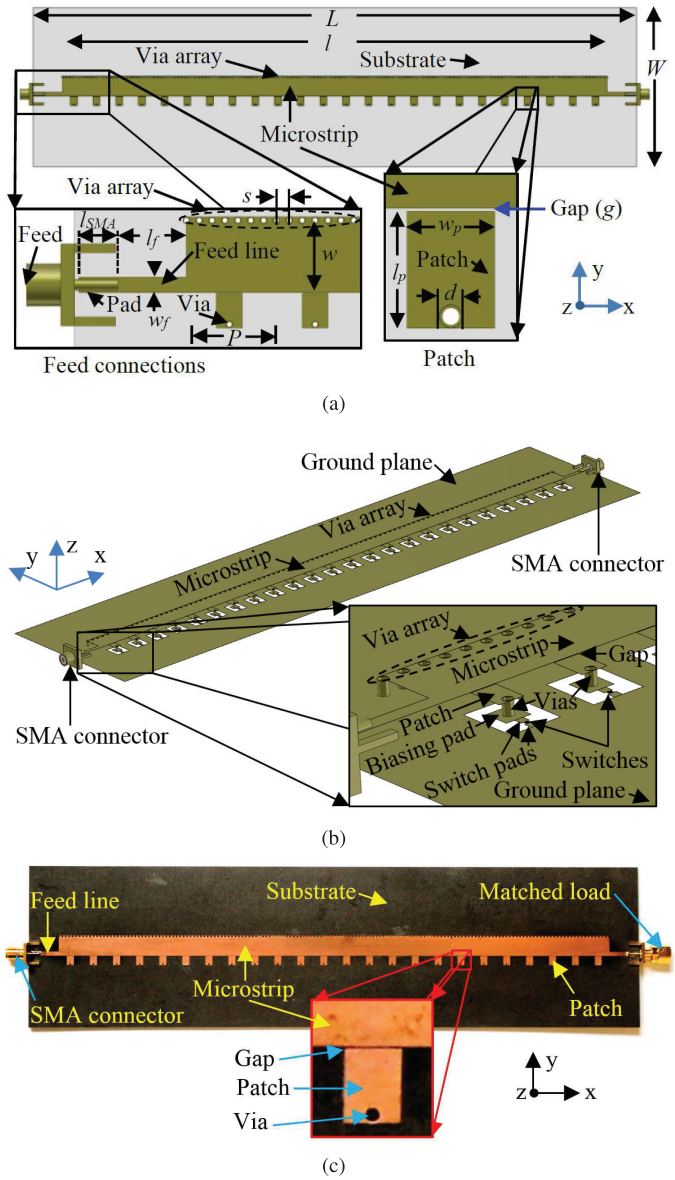


Fig. 2. Reconfigurable HW-MLWAs. (a) Top view. (b) Perspective view (substrate omitted, not to scale). (c) Top view of the antenna prototype.

a 0.5-mm gap between two switch pads to place the switching device. One terminal of the switch is connected to the biasing pad through a switch pad, while the other terminal is connected to the ground plane through the other switch pad. As the biasing pads are isolated from the microstrip and the ground plane, for dc, they provide the flexibility to control each switch independently. To prove the concept, ideal switches were used first in both simulations (PEC) and experiments (copper tape) to represent switches that are "ON" (1). The gap is left open to represent switches that are "OFF" (0). Effects of actual commercial switches are considered later.

To achieve good impedance matching for different macrocell states, different feed methods were investigated and their dimensions were optimized through parametric analyses conducted in CST. The best overall impedance matching for most of the states was found by feeding at the free edge of the microstrip with a uniform narrow feed line. The length ($l_f$)

and width ($w_f$) of the feed line are 8 and 1.8 mm, respectively. To connect the SMA connector pin, a small pad with a length ($l_{SMA}$) of 4.5 mm and width of 1.8 mm is printed [Fig. 2(a)], leaving a gap of 0.5 mm from the side of the substrate. A similar matching line and pad are provided at the other end of the microstrip to connect a matched load. The SMA connectors were modeled in the simulations according to the dimensions of a commercially available SMA connector, and the left connector was excited by a waveguide port in CST.

One antenna prototype is shown in Fig. 2(c). The antenna is fed from one end, and the other end of the antenna is terminated by a 50 Ω coaxial load to suppress any reflected waves. There are 161 vias (outer diameter of $d$) to short the upper edge of the microstrip to the ground plane. The center-to-center spacing ($s$) between two adjacent vias is 1.5 mm.

A uniform HW-MLWA was also considered for comparison. That antenna consists of a microstrip line with one edge shorted to the ground plane by an array of vias and a feed line at each end. The dimensions of the uniform HW-MLWA are the same as the dimensions of the prototyped antenna. The periodic patches, connecting vias, biasing pads, and the switches are absent in the uniform antenna.

## IV. Macrocell States of the LWA

There is a total of 24 binary unit cells in the antenna, i.e., N = 24. The characteristics of the antenna were investigated for different macrocell states. All possible CBPs applied to the antenna corresponding to macrocell orders from 1 to 4 are given in Table I. For N = 24, the possible orders of macrocells (M) are 1, 2, 3, 4, 6, 8, and 12. For example, M = 2 represents that a pair of adjacent unit cells are considered as a macrocell, and hence, the whole structure is configured with 12 such macrocells.

To analyze the antenna, multistate macrocells with orders (M) of 1, 2, 3, 4, 6, and 8 were considered. It does not require much effort to note that M = 8 covers all the states produced by M = 1, 2, and 4. Similarly, M = 6 covers all the states produced by M = 1, 2, and 3. This makes a total of 314 ($= 2^8 + 2^6 - 2^2 - 2^1$) different states for M = 1, 2, 3, 4, 6, and 8, after removing duplicated M = 1 and M = 2 states in the sum of M = 8 and M = 6 states. The antenna characteristics were investigated for all these macrocell states.

For M = 4, there exists a total of $2^4$ = 16 different macrocell states and, hence, 16 different CBPs as given in Table I. Of these 16 CBPs, a return loss greater than 10 dB is obtained at 6 GHz for 7 CBPs. The predicted radiation patterns for the four selected macrocell states of order M = 4 are shown in Fig. 3 together with two other patterns of a higher order (M = 8) macrocell. It confirms that not all macrocell states provide a unique beam angle. As expected, the main beams of the macrocell states M4(5) and M4(10) are similar, pointing at 48.5° and 49°, respectively, due to the identical EM properties of these macrocell states in an infinite structure. Similarly, the main beams produced by M4(1), M4(2), and M4(8) states are almost the same, all pointing at 55° as shown in Fig. 4. For the other two macrocell states, M4(0) and M4(15), the beams point at 63° and 32°, respectively. There are several different CBPs that can produce a main beam in the same direction.

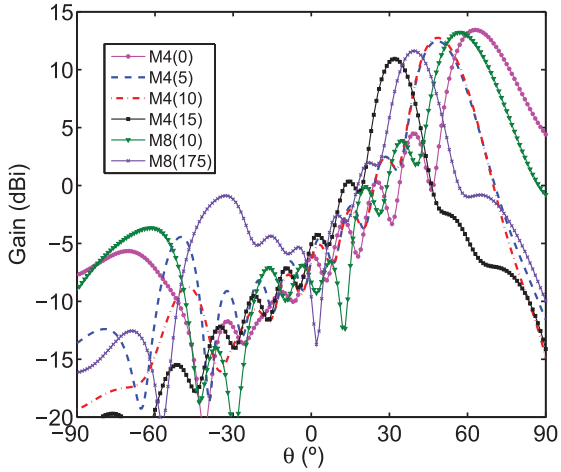


Fig. 3. Predicted radiation patterns of the reconfigurable HW-MLWA for six macrocell states (N = 24).

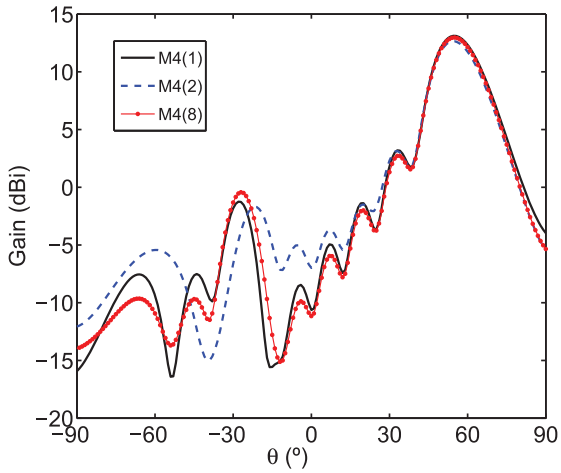


Fig. 4. Predicted very similar radiation patterns of the reconfigurable HW-MLWA for three macrocell states (N = 24).

For example, M4(5) and M2(2) [which is identical to M4(10)] states produce similar beams. However, the input reflection coefficients corresponding to M4(5) and M2(2) are significantly different: −11.7 and −19.6 dB, respectively. For intermediate beam directions, CBPs have been chosen considering best input impedance matching, i.e., M2(2) has been selected in this case. Like in conventional LWAs, the gain increases gradually as the beam scans toward endfire (i.e., as $\theta$ increases). The increase of gain with scanning angle is described later.

Five different CBPs were selected out of macrocell orders M = 1, 2, 3, 4, 6, and 8 to observe beam scanning at 6 GHz. The CBPs corresponding to the minimum and maximum beam angles were obtained for macrocell states M1(1) and M1(0), when all the switches are "1" and "0," respectively (these states are identical to M4(15) and M4(0), respectively). Three intermediate CBPs were selected from the remaining 312 macrocell states, considering input matching, gain, and desired beam directions. They are M1(0), M1(1), M2(2) [= M4(10)], M8(10), and M8(175), and their patterns are shown in Fig. 3. It was found that these five independent beams are sufficient to fill in the beam scanning range of this antenna. All five selected

TABLE II
SELECTED MACROCELL STATES AND CORRESPONDING MAIN BEAM DIRECTIONS AT 6 GHZ

| Macro-cell state | CBP | Main beam directions | |
|---|---|---|---|
| | | Predicted | Measured |
| M1(1) | 1111111111111111111111111 (CBP1) | 32° | 31° |
| M8(175) | 10101111101011111010111 (CBP2) | 39° | 38° |
| M2(2) | 10101010101010101010101010 (CBP3) | 49° | 47° |
| M8(10) | 00001010000010100000101 0 (CBP4) | 57° | 53° |
| M1(0) | 0000000000000000000000000 (CBP5) | 63° | 60° |

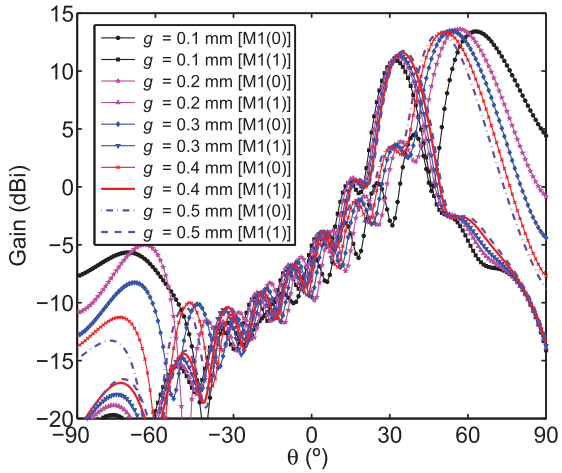


Fig. 5. Predicted radiation patterns of the reconfigurable HW-MLWA in the two extreme states of M1(0) and M1(1), for different values of the gap ($g$).

CBPs are listed in Table II, together with their predicted and measured main beam directions. The gain for some macrocell states is low, e.g., due to poor input matching, and those states have been excluded.

Although the antenna beam steering has been described here for operation at 6 GHz, the beam can be steered at other frequencies as well. Appropriate macrocell states need to be selected for the desired frequency, and the scanning limits will vary with the operating frequency, due to inherent nature of LWAs.

## V. ANTENNA PERFORMANCE

### A. Effect of Antenna Parameters on Scanning Range

The beam scanning range of the proposed antenna mainly depends on the capacitance of the gap between the microstrip edge and the patch [Fig. 2(a) right inset]. The capacitance of a gap capacitor decreases with an increase of gap $g$. Reduced gap capacitance decreases the beam scanning range. Fig. 5 highlights the effect of the gap $g$ on beam scanning range. The gap $g$ is varied between 0.1 and 0.5 mm. The best scanning range is obtained as expected for $g = 0.1$ mm. The beam scanning ranges for all five values of the gap are listed in Table III. The value of $g$ is chosen to be 0.1 mm.

The width ($w_p$) of the patch was varied to observe the effect of the gap capacitor length on the scanning range. It was found that when $w_p = 2$ mm, the main beam scanned between 30° and 60°, and with $w_p = 5$ mm, the scanning limits shifted to 36°–67°. Though the scanning range is almost the same for different lengths of gap capacitor, the beam scanning limits shift toward endfire for longer gap capacitors.

TABLE III
EFFECT OF GAP ON THE SCANNING RANGE

| Gap (mm) | Macro-cell state | Beam direction ($\theta$) | Scanning range |
|---|---|---|---|
| g = 0.1 | M1(0) | 63° | 31° |
| | M1(1) | 32° | |
| g = 0.2 | M1(0) | 57° | 24° |
| | M1(1) | 33° | |
| g = 0.3 | M1(0) | 54° | 20° |
| | M1(1) | 34° | |
| g = 0.4 | M1(0) | 51° | 16° |
| | M1(1) | 35° | |
| g = 0.5 | M1(0) | 49° | 14° |
| | M1(1) | 35° | |

Effect of the unit cell length ($P$) and microstrip width ($w$) on scanning range was also investigated. When $P = 8$ mm, i.e., 30 unit cells in the reconfigurable HW-MLWA, the antenna has a beam steering range of 30°–72°. However, the gain decreases in the upper scanning range due to poor radiation efficiency near endfire region. For $P = 12$ mm, i.e., 20 unit cells in the antenna, the beam steering range reduced to 34°–63°. Increase of the microstrip width ($w$) shifts the antenna operation to lower frequencies and vice versa. For example, when $w = 9$ mm, the main beam can be steered between 29° and 65° at 5.5 GHz with predicted gain greater than 10.5 dBi. When $w = 7$ mm, the main beam can be steered between 29° and 73° at 6.5 GHz with predicted gains at the smallest and largest beam angles are 9.8 and 10.7 dBi, respectively. A given antenna design can be scaled to other frequencies for other applications, and similar performance figures in matching, gain fluctuation, and steering range can be achieved in the new band using the same CBPs.

### B. Comparison Between Uniform and Reconfigurable HW-MLWA

As mentioned in Section III, a uniform HW-MLWA was modeled and analyzed for comparison. It has a 10 dB return loss of 2 GHz (5.47–7.47 GHz). The direction of the main beam is given by (1), where $\beta/k_0$ changes with frequency, so by sweeping the operating frequency, the main beam can be steered. At 5.5 GHz, the main beam is directed at 26°, and at 7 GHz, the beam is directed at 63°. In other words, 37° of beam scanning requires a frequency sweep of 1.5 GHz. Fig. 6(a) and (b) shows the current distribution of the uniform HW-MLWA at 5.66 GHz (main beam direction is at 32°) and 7 GHz (main beam direction is at 63°), respectively.

In frequency-scanning LWAs, more energy travels toward the load end with an increase of frequency. A similar effect is observed in the reconfigurable antenna at a fixed frequency when switching between different macrocell states. Fig. 6(c)–(e) represents the current distributions of the reconfigurable antenna at 6 GHz for CBP1 (M1(1) state), CBP3 (M2(2) state), and CBP5 (M1(0) state), respectively. They illustrate that when changing the CBPs from 1 to 5 to steer the beam toward endfire direction, the effective aperture length gradually increases, as

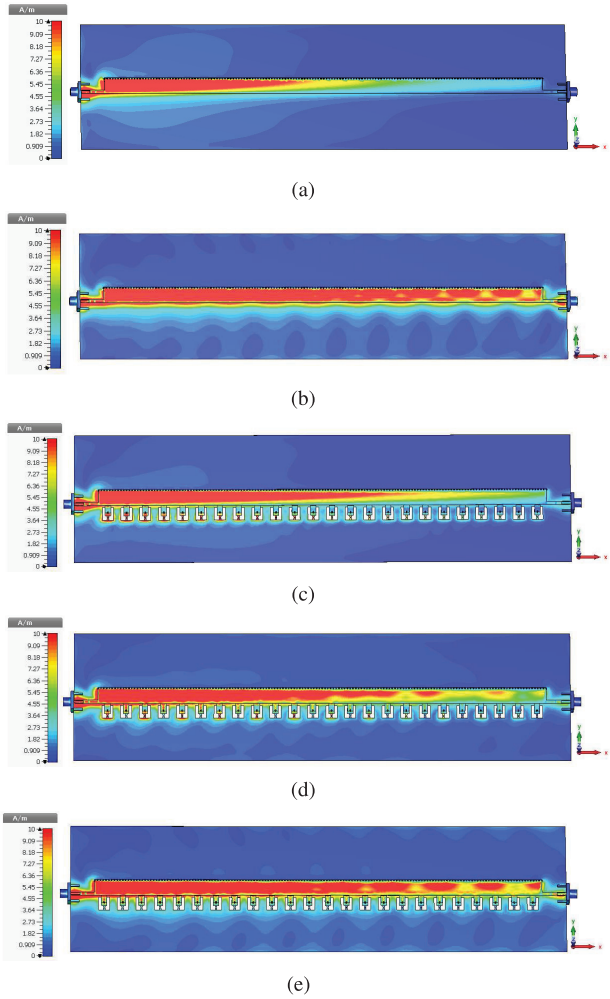


Fig. 6. Surface current distributions (amplitude) of two different antennas. (a) Uniform HW-MLWA at 5.66 GHz. (b) Uniform HW-MLWA at 7 GHz. (c) Reconfigurable HW-MLWA with CBP1 at 6 GHz. (d) Reconfigurable HW-MLWA with CBP3 at 6 GHz. (e) Reconfigurable HW-MLWA with CBP5 at 6 GHz.

in the case of the uniform LWA when increasing the operating frequency for the same purpose. It results in higher directivity for near-endfire directions. Since the gaps surrounding the biasing pads of the reconfigurable HW-MLWA are very narrow [Fig. 2(b)], back radiation from those gaps is negligible.

Radiation efficiency of an MLWA is high when the beam points close to the boresight, and it decreases when the beam move toward endfire [34]. The radiation efficiency of the uniform HW-MLWA gradually decreases by 23% from 97% to 74% when the main beam scans from 32° to 63°. On the other hand, the radiation efficiency of the reconfigurable HW-MLWA decreases only by 14.7% from 94.7% to 80%, when the beam scans the same range at 6 GHz. The total efficiency of the reconfigurable antenna is close to the radiation efficiency for all selected macrocell states, since the antenna is properly matched for all those states. The decrease in radiation efficiency compensates for the increase in directivity, when the beam is being steered toward end-fire direction in both types of LWAs. As a result, in a good LWA design, this gain variation can be made less than the industry standard 3 dB limit. For example, the variation of realized measured gain of our antenna prototype is only 1.2 dB Table IV.

TABLE IV
SELECTED MACROCELL STATES AND CORRESPONDING REFLECTION COEFFICIENT AND GAIN VALUES AT 6 GHZ

| CBP | Macro-cell state | $\|S_{11}\|$ (dB) | | | Gain (dBi) | |
|---|---|---|---|---|---|---|
| | | Predicted[1] | Predicted[2] | Measured | Predicted[1] | Measured |
| CBP1 | M1(1) | −14.2 | −15.9 | −11.1 | 11.8 | 11.7 |
| CBP2 | M8(175) | −14.6 | −14.2 | −11.8 | 11.9 | 12.1 |
| CBP3 | M2(2) | −19.6 | −16.6 | −14.3 | 13.1 | 12.1 |
| CBP4 | M8(10) | −13.8 | −10.5 | −13.6 | 13.4 | 12.5 |
| CBP5 | M1(0) | −23.8 | −17.5 | −17.1 | 14.4 | 12.9 |

[1]Ideal switches
[2]PIN diode equivalent circuit model.

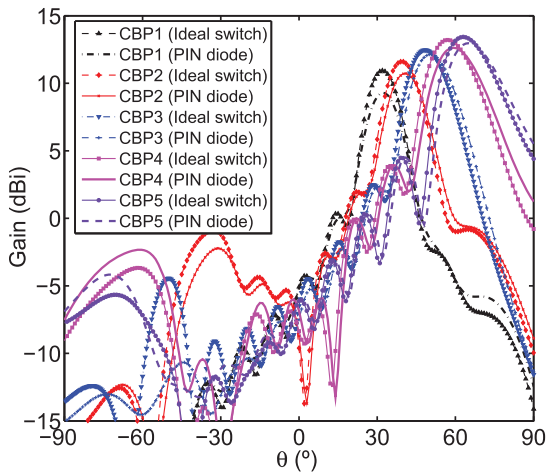


Fig. 7. Predicted radiation patterns of the reconfigurable HW-MLWA with ideal and actual switch parameters.

### C. Analysis of Reconfigurable HW-MLWA With Actual Switch Parameters

In order to verify the operation of the reconfigurable antenna in a real electronic environment, an investigation was conducted by incorporating parameters of a commercially available switch to the LWA model. GaAs MA4GP907 PIN diodes have been used extensively in reconfigurable antenna design, e.g., [35], [36]. Based on the MA4GP907 PIN diode datasheet [37] and previous research [36], the diode was modeled as a 4.2-Ω resistor for the "ON" state and a 0.025-pF capacitor for the "OFF" state in our simulations. Fig. 7 shows the radiation patterns of the reconfigurable MLWA with ideal switches and actual switches (MA4GP907 PIN diode), and the reflection coefficients at 6 GHz for both cases are listed in Table IV. Similar radiation patterns are obtained for both cases. As expected, the gain decreases when diode parameters are included. For CBP1, the main beam is directed at 32° in both cases. However, for CBP5, the main beam is directed at 63° and 65° in ideal and actual cases, respectively. In the actual case, the beam scanning range is slightly larger (33°), which attributed to the "OFF" state capacitance of the PIN diode. The change in return loss due to actual switches is not practically significant.

Since each switch is individually controlled, any number of macrocell states can be easily implemented in the antenna.

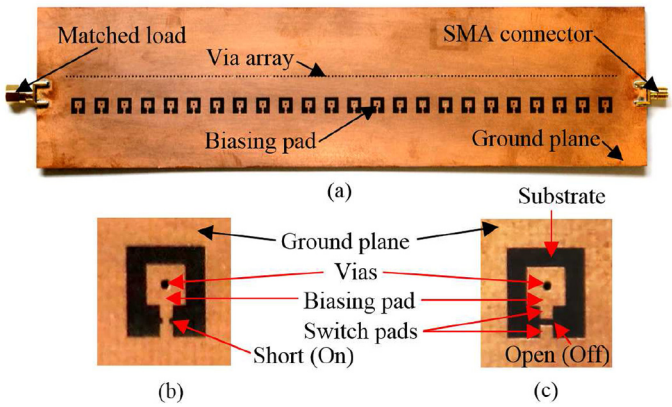


Fig. 8. Back view of the reconfigurable MLWA prototype. (a) Complete structure (CBP1). (b) "ON" state. (c) "OFF" state.

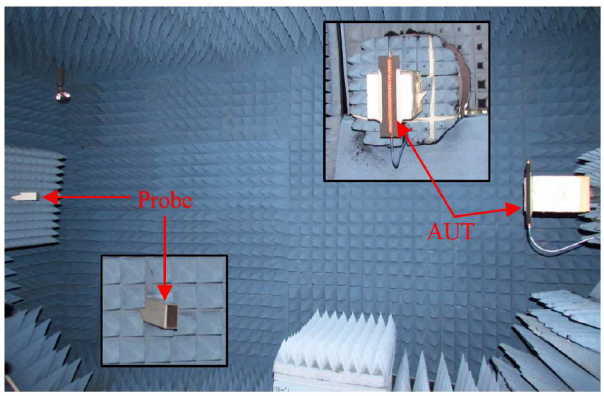


Fig. 9. Pattern measurement setup at the AusAMF.

## VI. Measured Results

### A. Reflection Coefficients

The input reflection coefficients of the antenna prototype in the five selected macrocell states were measured using an Agilent PNA-X N5242A network analyzer. Back views of the prototype and "ON"- and "OFF"-states of a switch are shown in Fig. 8. Different macrocell states and, hence, CBPs can be implemented by changing the switch states. The measured and predicted $|S_{11}|$ at 6 GHz in the selected states are listed in Table IV. The measured return loss is greater than 10 dB for all the selected macrocell states at 6 GHz.

### B. Radiation Patterns

The radiation characteristics were measured using the NSI700S-50 spherical near-field range at the Australian Antenna Measurement Facility (AusAMF). The antenna was placed vertically for the measurements, as shown in Fig. 9, to align it with the probe, since the antenna is polarized in the y-direction (Fig. 2). The measured x–z-plane (H-plane) radiation patterns at 6 GHz are shown in Fig. 10. By changing the macrocell states, the main beam can be steered in discrete steps between 31° and 60°.

For CBP1 (M1(1) state), the main beam direction at 6 GHz is closer to the boresight (exactly at 31°). By changing the macrocell state, the main beam is gradually scanned toward endfire at

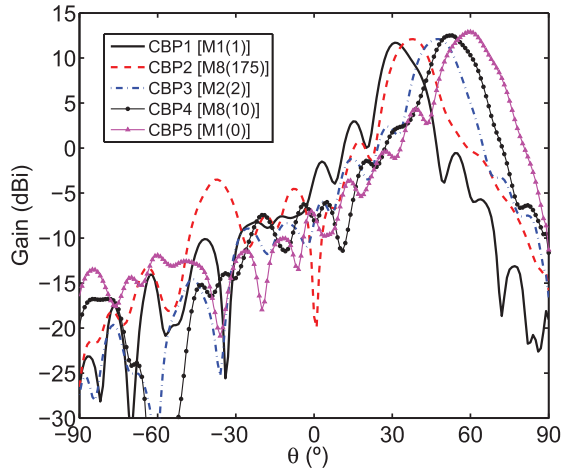


Fig. 10. Measured radiation patterns of the reconfigurable HW-MLWA on the x–z plane (H-plane) at 6 GHz for the selected macrocell states.

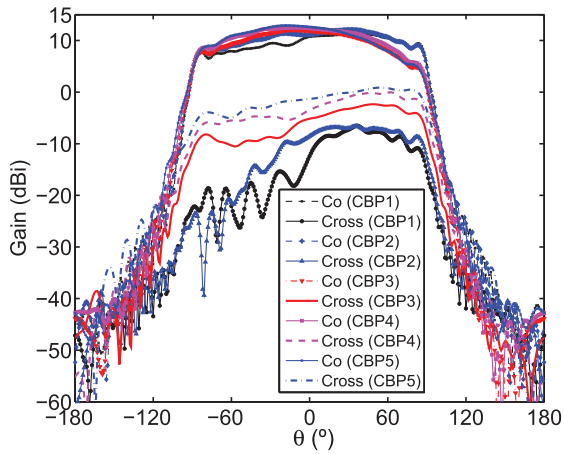


Fig. 11. Measured radiation patterns of the reconfigurable HW-MLWA on E-plane at 6 GHz for the selected macrocell states.

the same frequency (6 GHz). The predicted and measured directions of the main beam for different states are listed in Table II. Fig. 11 shows the measured E-plane radiation patterns at 6 GHz for the selected five macrocell states. It was observed that the cross-polarization level on x–z plane is below 14.2 dB for all CBPs.

### C. Measured Gain

Measured and predicted gains at 6 GHz for the five selected CBPs are listed in Table IV. The gain was measured using the gain comparison method. The maximum measured gain is 12.9 dBi at 6 GHz. Within the scanning range from 31° to 60°, the variation of the measured gain is only 1.2 dB.

The gain for CBP1 is lower compared to that for CBP5 as expected. The measured and predicted gains are 11.7 and 11.8 dBi, respectively, for CBP1, and they increase with the scanning angle.

## VII. Conclusion

A digital method to steer in steps the beam of periodic MLWAs at a fixed frequency, using only two DC bias voltage values, is presented. By loading the free edge of the microstrip

line with the periodic gap capacitors and controlling their connection to the ground plane by binary switches, beam scanning is achieved without changing the frequency and without lumped capacitors.

A multistate macrocell approach has been developed to analyze reconfigurable periodic structures, and it has been applied to design reconfigurable MLWAs. This approach helps to conduct the analysis and design of a reconfigurable periodic structure in a systematic fashion. Numerical full-wave analyses and experimental measurements have validated the concept. The measured scanning range of the prototyped antenna is 29° at 6 GHz. The peak measured gain at 6 GHz is 12.9 dBi, and its variation within the scanning range is only 1.2 dB.

## REFERENCES


[1] W. Menzel, "A new travelling wave antenna in microstrip," in *Proc. 8th Eur. Microw. Conf.*, Sep. 1978, pp. 302–306.

[2] H. Ermert, "Guiding and radiation characteristics of planar waveguides," *IEE Microw. Opt. Acoust.*, vol. 3, no. 2, pp. 59–62, Mar. 1979.

[3] A. A. Oliner, "Leakage from higher modes on microstrip line with application to antennas," *Radio Sci.*, vol. 22, no. 6, pp. 907–912, 1987.

[4] D. R. Jackson, A. A. Oliner, "Leaky-wave antennas," in Modern Antenna Handbook, C. A. Balanis, Ed. Hoboken, NJ, USA: Wiley, 2008, ch. 7.

[5] D. R. Jackson, C. Caloz, and T. Itoh, "Leaky-wave antennas," *Proc. IEEE*, vol. 100, no. 7, pp. 2194–2206, Jul. 2012.

[6] D. K. Karmokar, K. P. Esselle, and T. S. Bird, "An array of half-width microstrip leaky-wave antennas radiating on boresight," *IEEE Antennas Wireless Propag. Lett.*, vol. 14, pp. 112–114, Jan. 2015.

[7] Q. Lai, C. Fumeaux, and W. Hong, "Periodic leaky-wave antennas fed by a modified half-mode substrate integrated waveguide," *IET Microw., Antennas Propag.*, vol. 6, no. 5, pp. 594–601, Apr. 2012.

[8] S. K. Podilchak, A. P. Freundorfer, and Y. M. M. Antar, "Broadside radiation from a planar 2-D leaky-wave antenna by practical surface-wave launching," *IEEE Antennas Wireless Propag. Lett.*, vol. 7, pp. 517–520, Dec. 2008.

[9] T.-L. Chen, Y.-D. Lin, and J.-W. Sheen, "Microstrip-fed microstrip second higher order leaky-mode antenna," *IEEE Trans. Antennas Propag.*, vol. 49, no. 6, pp. 855–857, Jun. 2001.

[10] C. Caloz, D. R. Jackson, and T. Itoh, "Leaky-wave antennas," in Frontiers in Antennas, F. B. Gross, Ed. New York, NY, USA: McGraw-Hill, 2011, ch. 9.

[11] L. Liu, C. Caloz, and T. Itoh, "Dominant mode leaky-wave antenna with backfire-to-endfire scanning capability," *Electron. Lett.*, vol. 38, no. 23, pp. 1414–1416, Nov. 2002.

[12] G. M. Zelinski, G. Thiele, M. L. Hastriter, M. J. Havrilla, and A. Terzuoli, "Half width leaky wave antennas," *IET Microw., Antennas Propag.*, vol. 1, no. 2, pp. 341–348, Apr. 2007.

[13] J. Liu, D. R. Jackson, Y. Li, C. Zhang, and Y. Long, "Investigations of SIW leaky-wave antenna for endfire-radiation with narrow beam and sidelobe suppression," *IEEE Trans. Antennas Propag.*, vol. 62, no. 9, pp. 4489–4497, Sep. 2014.

[14] N. Nasimuddin, Z. N. Chen, and X. Qing, "Multilayered composite right/left-handed leaky-wave antenna with consistent gain," *IEEE Trans. Antennas Propag.*, vol. 60, no. 11, pp. 5056–5062, Nov. 2012.

[15] C. Jin and A. Alphones, "Leaky-wave radiation behavior from a double periodic composite right/left-handed substrate integrated waveguide," *IEEE Trans. Antennas Propag.*, vol. 60, no. 4, pp. 1727–1735, Apr. 2012.

[16] G.-F. Cheng and C.-K. C. Tzuang, "A differentially excited coupled half-width microstrip leaky $EH_1$ mode antenna," *IEEE Trans. Antennas Propag.*, vol. 61, no. 12, pp. 5885–5892, Dec. 2013.

[17] N. Yang, C. Caloz, and K. Wu, "Full-space scanning periodic phase-reversal leaky-wave antenna," *IEEE Trans. Microw. Theory Techn.*, vol. 58, no. 10, pp. 2619–2632, Oct. 2010.

[18] N. Nguyen-Trong, T. Kaufmann, and C. Fumeaux, "A wideband omnidirectional horizontally polarized traveling-wave antenna based on half-mode substrate integrated waveguide," *IEEE Antennas Wireless Propag. Lett.*, vol. 12, pp. 682–685, May 2013.

[19] Y. Li, Q. Xue, H.-Z. Tan, and Y. Long, "The half-width microstrip leaky wave antenna with the periodic short circuits," *IEEE Trans. Antennas Propag.*, vol. 59, no. 9, pp. 3421–3423, Sep. 2011.

[20] A. P. Saghati, M. M. Mirsalehi, and M. H. Neshati, "A HMSIW circularly polarized leaky-wave antenna with backward, broadside, and forward radiation," *IEEE Antennas Wireless Propag. Lett.*, vol. 13, pp. 451–454, Mar. 2014.

[21] N. Nasimuddin, Z. N. Chen, and X. Qing, "Substrate integrated metamaterial-based leaky-wave antenna with improved boresight radiation bandwidth," *IEEE Trans. Antennas Propag.*, vol. 61, no. 7, pp. 3451–3457, Jul. 2013.

[22] Y. Mohtashami and J. Rashed-Mohassel, "A butterfly substrate integrated waveguide leaky-wave antenna," *IEEE Trans. Antennas Propag.*, vol. 62, no. 6, pp. 3384–3388, Jun. 2014.

[23] S.-T. Yang and H. Ling, "Design of a microstrip leaky-wave antenna for two-dimensional bearing tracking," *IEEE Antennas Wireless Propag. Lett.*, vol. 10, pp. 784–787, Aug. 2011.

[24] J. Liu, D. R. Jackson, and Y. Long, "Substrate integrated waveguide (SIW) leaky-wave antenna with transverse slots," *IEEE Trans. Antennas Propag.*, vol. 60, no. 1, pp. 20–29, Jan. 2012.

[25] M. Archbold, E. Rothwell, L. C. Kempel, and S. W. Schneider, "Beam steering of a half-width microstrip leaky-wave antenna using edge loading," *IEEE Antennas Wireless Propag. Lett.*, vol. 9, pp. 203–206, Apr. 2010.

[26] C. Luxey and J.-M. Laheurte, "Effect of reactive loading in microstrip leaky wave antennas," *Electron. Lett.*, vol. 36, no. 15, pp. 1259–1260, Jul. 2000.

[27] J. Liu and Y. Long, "Analysis of a microstrip leaky-wave antenna loaded with shorted stubs," *IEEE Antennas Wireless Propag. Lett.*, vol. 7, pp. 501–504, Dec. 2008.

[28] G. Augustin, S. V. Shynu, C. K. Aanandan, P. Mohanan, and K. Vasudevan, "A novel electronically scannable log-periodic leaky-wave antenna," *Microw. Opt. Technol. Lett.*, vol. 45, no. 11, pp. 163–165, Apr. 2005.

[29] Y. Li and Y. Long, "Frequency-fixed beam-scanning microstrip leaky-wave antenna with multi-terminals," *Electron. Lett.*, vol. 42, no. 1, pp. 7–8, Jan. 2006.

[30] R. Guzman-Quiros, J. L. Gomez-Tornero, A. R. Weily, and Y. J. Guo, "Electronically steerable 1-D Fabry-Perot leaky-wave antenna employing a tunable high impedance surface," *IEEE Trans. Antennas Propag.*, vol. 60, no. 11, pp. 5046–5055, Nov. 2012.

[31] R. Ouedraogo, E. Rothwell, and B. Greetis, "A reconfigurable microstrip leaky-wave antenna with a broadly steerable beam," *IEEE Trans. Antennas Propag.*, vol. 59, no. 8, pp. 3080–3083, Aug. 2011.

[32] S. Lim, C. Caloz, and T. Itoh, "Electronically scanned composite right/left handed microstrip leaky-wave antenna," *IEEE Microw. Wireless Compon. Lett.*, vol. 14, no. 6, pp. 277–279, Jun. 2004.

[33] Z. L. Ma, L. J. Jiang, S. Gupta, and W. E. I. Sha, "Dispersion characteristics analysis of one dimensional multiple periodic structures and their applications to antennas," *IEEE Trans. Antennas Propag.*, vol. 63, no. 1, pp. 113–121, Jan. 2015.

[34] D. K. Karmokar and K. P. Esselle, "Periodic U-slot-loaded dual-band half-width microstrip leaky-wave antennas for forward and backward beam scanning," *IEEE Trans. Antennas Propag.*, vol. 63, no. 12, pp. 5372–5381, Dec. 2015.

[35] E. Carrasco, M. Barba, and J. A. Encinar, "X-band reflectarray antenna with switching-beam using PIN diodes and gathered elements," *IEEE Trans. Antennas Propag.*, vol. 60, no. 12, pp. 5700–5708, Dec. 2012.

[36] M. Li, S.-Q. Xiao, Z. Wang, and B.-Z. Wang, "Compact surface-wave assisted beam-steerable antenna based on HIS," *IEEE Trans. Antennas Propag.*, vol. 62, no. 7, pp. 3511–3519, Jul. 2014.

[37] M/A-COM Technology Solutions. [Online]. Available: http://cdn.macom.com/datasheets/MA4GP907.pdf


**Debabrata K. Karmokar** (S'12–M'15) was born in Satkhira, Bangladesh. He received the B.Sc. degree in electrical and electronic engineering (EEE) from the Khulna University of Engineering and Technology (KUET), Khulna, Bangladesh, in 2007; and the Ph.D. degree in electronic engineering from the Macquarie University, Sydney, Australia, in 2015.

In 2007, he joined the Department of Electrical and Electronic Engineering, KUET, as a Lecturer and became an Assistant Professor in 2011. He was an Assistant Director of Students' Welfare of KUET where he was responsible for different administrative activities of the university, and a Member of Consultancy, Research and Testing Services (CRTS) of the Department of EEE, KUET. He has authored/co-authored more than 55 journal and conference papers. His research interests include leaky-wave antennas

(LWAs), metamaterial-based antennas, reconfigurable antennas, ultrawideband (UWB) antennas, broadband and multiband printed antennas, electromagnetic band gap (EBG) resonator antennas, dielectric-resonator antennas, and wireless power transfer.

Dr. Karmokar was a Secretary of the IEEE Student Branch, Macquarie University. He is serving as a Reviewer for several journals including the *IEEE Antennas and Wireless Propagation Letters* and the *IET Microwaves, Antennas and Propagation*. He was the recipient of a Commonwealth-Funded International Postgraduate Research Scholarship (IPRS) and an International Macquarie University Research Excellence Scholarship (iMQRES) from Macquarie University, an OCE Ph.D. Scholarship from the Commonwealth Scientific and Industrial Research Organisation (CSIRO) ICT Centre, Marsfield, Australia, and won the First Prize in Poster Competition in Engineering Symposium 2015, Macquarie University. His biography has been included in *Marquis Who's Who in the World* 2016 (33rd edition).

**Karu P. Esselle** (M'92–SM'96–F'16) received the B.Sc. degree (with first class Hons.) in electronic and telecommunication engineering from the University of Moratuwa, Moratuwa, Sri Lanka; and the M.A.Sc. and Ph.D. degrees in electrical engineering from the University of Ottawa, Ottawa, ON, Canada.

He is a Professor of Electronic Engineering with the Macquarie University, Sydney, Australia, and the Past Associate Dean—Higher Degree Research (HDR) of the Division of Information and Communication Sciences. He has authored around 450 research publications and his papers have been cited more than 3300 times. His current Google Scholar h-index of 29 is the all-time highest among Australian antenna researchers, when Google Scholar errors are corrected. Since 2002, his research team has been involved with research grants, contracts and PhD scholarships worth over 15 million dollars.

Prof. Esselle has served as a member of the Dean's Advisory Council and the Division Executive from 2003 to 2008 and as the Head of the department several times. He is the Chair of the Board of management of Australian Antenna Measurement Facility, the Deputy Director (Engineering) of the WiMed Research Centre, and elected as the 2016 Chair of both IEEE New South Wales (NSW) Section, and IEEE NSW AP/MTT Chapter. He directs the Centre for Collaboration in Electromagnetic and Antenna Engineering. When he was elected to the IEEE Antennas and Propagation Society Administrative Committee for a three-year term in 2014, he became the only person residing in the Asia-Pacific Region (IEEE Region 10) to be elected to this highly competitive position over a period of at least six years (2010–2015). He was elevated to IEEE Fellow grade for his extensive contributions to resonance-based antennas, both low-gain and high-gain. He has been invited to serve as an International Expert/Research Grant Assessor by several nationwide research funding bodies overseas including the Netherlands, Canada, Finland, Hong-Kong, Georgia, and Chile. He is an Associate Editor of the IEEE ACCESS and *IET Microwave, Antennas, and Propagation*. He is the Technical Program Committee Co-Chair of ISAP 2015, APMC 2011, and TENCON 2013, and the Publicity Chair of ICEAA 2016, IWAT 2014, and APMC 2000. He is the Foundation Counsellor of the IEEE Student Branch at Macquarie University, and the Foundation Advisor of IEEE MTT Chapter in Macquarie University. He has been invited by the Vice-Chancellors of Australian and overseas universities to assess applications for promotion to professorial levels. He has also been invited to assess grant applications submitted to Australia's most prestigious schemes such as Australian Federation Fellowships and Australian Laureate Fellowships. He leads the Implantable Wireless Program of the WiMed Research Centre. In addition to the large number of invited conference speeches he has given, he has been an Invited Keynote Speaker of IEEE workshops and conferences. He has provided expert assistance to more than a dozen companies including Intel, Hewlett Packard Laboratory (USA), Cisco Systems (USA), Cochlear, Optus, ResMed, and Katherine-Werke (Germany). His research has been funded by many national and international organizations including Australian Research Council, Intel, US Air Force, Cisco Systems and Hewlett-Packard, and Australian and Indian governments. His mentees have been awarded many fellowships, awards, and prizes for their research achievements. Thirty-one international experts who examined the theses of his recent Ph.D. graduates ranked them in the top 5% or 10%. He was the recipient of the 2012 Best Published Paper Award in Electronic and Telecommunication Engineering from IESL NSW Chapter, the 2011 Outstanding Branch Counsellor Award from IEEE headquarters (USA), the 2009 Vice Chancellor's Award for Excellence in Higher Degree Research Supervision, and the 2004 Inaugural Innovation Award for Best Invention Disclosure.

**Stuart G. Hay** (SM'10) received the B.E. and Ph.D. degrees in electrical engineering from the University of Queensland, Brisbane, Australia, in 1985 and 1994, respectively.

From 1986 to 1989 and since 1994, he has been with CSIRO, Sydney, Australia, where he is currently a Principal Research Scientist. His research interests include electromagnetics and antennas, including analysis and design techniques for reflectors and feeds, antenna arrays, impulse antennas, shapedbeam, multibeam, and beam-scanning antennas.

Dr. Hay served as an Associate Editor of the IEEE TRANSACTIONS ON ANTENNAS AND PROPAGATION from 2008 to 2013. He was a Guest Editor of a special issue of this journal, on Antennas for Next Generation Radio Telescopes. Since 2009, he has been the Chair of the Technical Program Committee of the Australian Symposium on Antennas.